Electrical and Computer Engineering Faculty Research & Creative Works

Electrical and Computer Engineering

01 May 2004

Susceptibility Characterization of a Cavity with an Aperture by using Slowly Rotating EM Fields: FDTD Analysis and Measurements

Kimitoshi Murano

Takeshi Sanpei

Fengchao Xiao

Chen Wang

et. al. For a complete list of authors, see https://scholarsmine.mst.edu/ele_comeng_facwork/1285

Susceptibility Characterization of a Cavity With an Aperture by Using Slowly Rotating EM Fields: FDTD Analysis and Measurements

Kimitoshi Murano, *Member, IEEE*, Takeshi Sanpei, Fengchao Xiao, *Member, IEEE*,
Chen Wang, *Student Member, IEEE*, Yoshio Kami, *Member, IEEE*, and James L. Drewniak, *Senior Member, IEEE*

Abstract—This paper describes the evaluation of the susceptibility of a cavity with an aperture using the finite-difference time-domain (FDTD) method and experimentally. To reduce the computing time, the FDTD method is used for the radiation from the cavity and the susceptibility is obtained by using the reciprocity theorem. The cavity used here is modeled after a full-tower desktop enclosure with a 3.5-in bay. The susceptibility characteristics are evaluated by measuring outputs of a monopole antenna and transmission lines installed in the cavity. The susceptibility characteristics, using a three-dimensional (3-D) map, are studied from the computed and the measured results by applying slowly rotating electromagnetic fields to the cavity on a turntable. Measured and modeled results are in good agreement, indicating the merits of the proposed approach for susceptibility/immunity evaluation. Moreover, some discussions are made to check the susceptibility mechanism.

Index Terms—Electromagnetic coupling, finite-difference time-domain (FDTD) method, reciprocity theorem, rotating fields, three-dimensional (3-D) susceptibility map.

I. INTRODUCTION

THE GROWING proliferation of electronic and electrical systems creates an increasingly more severe electromagnetic environment for electronic equipment and makes immunity to various types of electromagnetic interference more critical. Putting an electronic product in a metallic shielding enclosure to reduce the equipment susceptibility, although an old idea, remains a commonly used method. Considerable work has been done on the electromagnetic characteristics of the metallic shield based on shielding effectiveness evaluation. Analytical or semi-analytical techniques provide a closed-form solution [1]–[3], allowing for fast calculations, but are limited to cases with simple geometries. Numerical techniques, such as the finite-difference time-domain (FDTD) method [4], [5], the methods of moments (MoM) [6], or a hybrid approach of FDTD and MoM [7], require more computation cost than

analytical techniques, but they calculate the problem based on a full-wave analysis, and thus, are very powerful analysis tools. The state-of-the-art in numerical modeling of metallic enclosures is advancing at a rapid pace, and a thorough list of publications can be overwhelming. Some of the recent contributions can be found in the references given in [7] and [8]. A variety of practical techniques for the design of shielding enclosures can be found in a design book by Gnecco [9].

For checking the susceptibility of equipment, various standard test facilities such as a semi-anechoic chamber, transverse electromagnetic (TEM) and gigahertz-TEM (GTEM) cells, a reverberation chamber, etc., are commonly used. To measure the susceptibility characteristics of the equipment for electromagnetic fields in different specific polarizations, however, the equipment must be mechanically rotated. When a reverberation chamber is employed, the field-polarization information is even unknown. Recently, a new susceptibility test method using electromagnetic (EM) fields with a low rate of rotation, rotating fields, has been proposed [10]. Since the EM fields incident on an equipment under test (EUT) are always controlled, the susceptibility of the EUT to external fields in various directions and polarizations may be assessed electronically and continuously within a considerably short time.

In this paper, the susceptibility of a cavity with an aperture is investigated using slowly rotating EM fields. Shielding effectiveness (SE) is most commonly used for evaluating the shielding capability of the enclosure. For the electric field (E-field), SE is defined as

$$\mathrm{SE} = -20\log_{10}\frac{|\boldsymbol{E}|}{|\boldsymbol{E}_0|} \qquad (1)$$

where $\boldsymbol{E}_0$ and $\boldsymbol{E}$ are the E-field without and with shielding, respectively. The electric fields $\boldsymbol{E}_0$ and $\boldsymbol{E}$ depend on the arrangement positions of a field sensor, and SE is in fact the ratio between the two field strengths. On the other hand, susceptibility is determined only by the electric field $\boldsymbol{E}$. Significant susceptibility to an external field may result, even if the SE is high. Therefore, the shielding capability of the cavity is evaluated by using the susceptibility in this paper. Both the empty cavity and the cavity with a victim circuit inside are investigated. For each case, the three-dimensional (3-D) susceptibility characteristics are measured using rotating EM fields in an anechoic chamber. The numerical method used for the analysis is the FDTD method [11]. The FDTD method is a versatile method and has been extensively used in solving many classes of EM
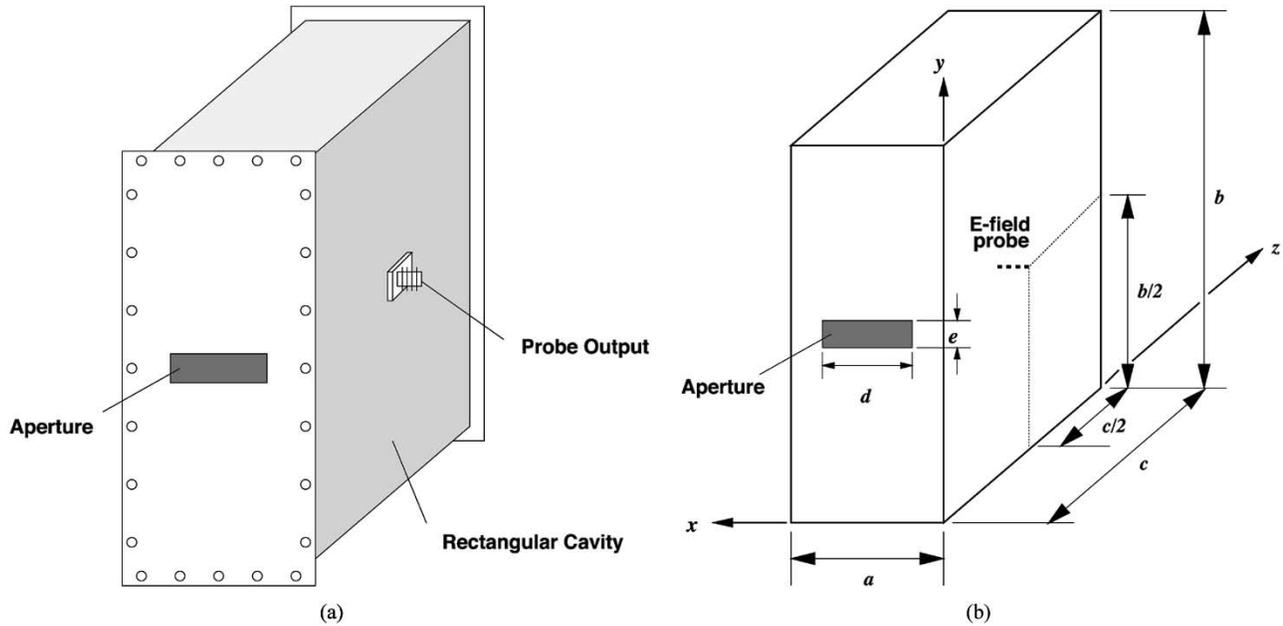
Fig. 1. Geometry of the rectangular cavity with an aperture. (a) Overview. (b) Coordinates and dimensions.

problems. If the FDTD method is applied directly to model the rotating EM fields and evaluate the 3-D susceptibility characteristics, the simulation time would be large since the direction and the polarization of the incident wave on the cavity are continuously changed. The computation cost easily gets out of hand. To overcome this difficulty, the reciprocity theorem is employed in the FDTD analysis. Instead of modeling the rotating fields incident from outside the cavity, the input of the FDTD modeling is located in the interior, where the susceptibility is measured in the experiments. Then the far fields are calculated based on the near-zone to far-zone transformation. These far fields quantitatively indicate the susceptibility characteristics. Hence, the 3-D susceptibility characteristics can be obtained in only one FDTD run, and the computation requirements dramatically decreased. To ascertain the susceptibility mechanism related to the victim circuit in the cavity, the modified telegrapher's equations are applied to the model herein [12]–[15].

II. NUMERICAL AND EXPERIMENTAL METHOD OF SUSCEPTIBILITY EVALUATION WITH SLOWLY ROTATING FIELDS

A. Model

The cavity with an aperture examined here models the chassis of a tower-type desktop personal computer as shown in Fig. 1. An aperture is located in the center of the cavity front wall. The aperture models an insertion opening of a peripheral device to the internal space of the chassis denoted a "3.5-in bay." An insertion opening is merely an aperture when the peripheral device is not installed. The EM fields inside the cavity couple with the external EM fields through the aperture in the cavity.

The cavity is made from aluminum plates, and the internal size is $a \times b \times c = 180 \times 420 \times 440$ mm. The thickness of the cavity wall is 0.5 mm. The cavity resonates at a frequency of 492 MHz for the dominant TE_{011} mode. The separation between the TE_{011} mode and the next lowest mode (TE_{101}) is

greater than 400 MHz. The size of the aperture is almost equal to the size of the insertion opening to a bay, with dimensions of $d \times e = 100 \times 25$ mm.

The field magnitude inside the cavity is measured using an electric-field monopole probe attached in the cavity side wall. The output of the probe is evaluated as the susceptibility characteristic of the cavity. In addition, the case where a transmission line is stretched in the cavity is also examined.

The susceptibilities of EUTs are determined experimentally by using the rotating-EM-field method [10]. This method uses an EM field rotating in a plane at a very low rate (e.g., less than 1 Hz). Using this approach for susceptibility evaluation, the susceptibility characteristics of the EUT for the entire polarization can be determined in detail and automatically. This is denoted the susceptibility map hereafter.

B. FDTD Analysis Using the Reciprocity Theorem

The FDTD method is a direct solution of Maxwell's time-dependent curl equations, based on simple central-difference approximations to evaluate the space and time derivatives. The incident wave source in the FDTD modeling is a time-sampled analog signal excited at a specific point or on a specific plane, and usually also in a specific direction. The computation region is discretized into the so-called Yee-cells, and the electric and magnetic fields are evaluated based on a leapfrog time-stepping process. If the FDTD method is applied directly to evaluate the 3-D susceptibility characteristics of the aforementioned model, the computation cost would be overwhelming, since for each direction and polarization of the incident field, the FDTD modeling should be executed one time. Here, the reciprocity theorem is used to resolve this problem. The reciprocity theorem is a basic law of nature and often used in circuit theory and antennas. In the simplest sense, the reciprocity theorem states, that a response of a circuit system to a source is unchanged when source and measurement are interchanged. A cavity can be viewed as
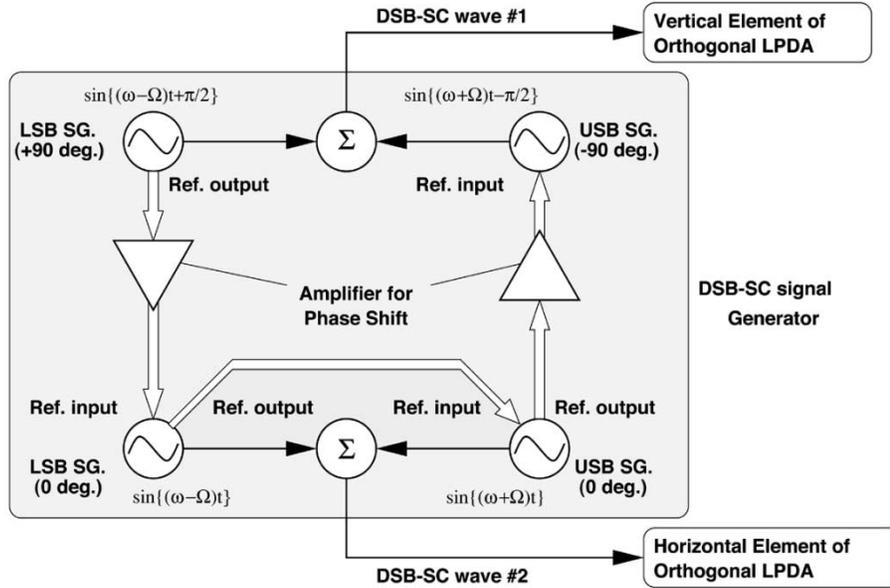
Fig. 2.   Block diagram of the generation system of the rotating EM field.

a circuit with the source at one side of the cavity and outputs at the other. As long as the cavity can be considered to be a passive and linear system, the reciprocity theorem holds, and the input and output in the FDTD modeling can be interchanged. Therefore, the input of the FDTD modeling is placed in the cavity interior, where the susceptibility is evaluated in the experiments, instead of modeling the rotating fields coming from the exterior of the cavity. Then the electric and magnetic fields on a virtual surface completely surrounding the FDTD model of the cavity are calculated. From the calculated values of these fields on the surface, equivalent electric and magnetic surface current distributions are determined and the far fields (4 m away from the cavity in our experiments) are extracted based on the near-zone to far-zone transformation [4],[11]. These far fields quantitatively indicate the susceptibility characteristics. Since the 3-D susceptibility characteristics can be obtained in only one FDTD run, the computation requirements are greatly decreased. The calculated susceptibility characteristics over the polarization angle are obtained by combining the two orthogonal FDTD components of the far fields.

In the following FDTD modeling, a cell size of $0.5 \times 0.5 \times 0.5$ cm is used. Since the thickness of the wall is small compared with wavelength, it is not taken into consideration. The cavity walls are modeled as perfect electric conductors by setting the tangential electric field to zero. The excitation of the probe is modeled by a voltage source with a 50-Ω resistance in a single cell at the feeding point. The victim circuit, a wire in our experiments, is modeled with the commonly used thin wire algorithm [11].

C. Experimental Setup

The experimental setup is shown in Fig. 2. Two different double-side-band, suppressed-carrier (DSB-SC) waves that are necessary to generate the rotating-EM fields are synthesized

using four signal generators (SGs). By exciting an orthogonal log-periodic dipole-array antenna (LPDA) with the above two DSB-SC waves, the rotating-EM fields are generated in an anechoic chamber. The fields radiated from the orthogonal LPDA rotate in a vertical plane (x–y plane) two dimensionally in the anechoic chamber. A schematic of the test setup is shown in Fig. 3. The EUT is irradiated with the rotating-EM fields with the orthogonal LPDA separated from the EUT by 4 m as shown in Fig. 4. Furthermore, the susceptibility characteristics of the EUT over the azimuth, θ, can be measured by putting it on a turntable. Then, the 3-D susceptibility characteristics (3-D susceptibility map) can be measured. The susceptibility is here defined as an output power of the probe or transmission-line terminal when an incident E-field of 1 V/m is applied to the EUT. The incident E-field is monitored by using a half-wave dipole antenna located near the EUT. It was checked that there was no influence of any currents on the attached cable. Thus, the common-mode chokes are not put on the attached cable.

III. NUMERICAL AND EXPERIMENTAL RESULTS

To estimate the susceptibility of the cavity with an aperture, the internal EM field of the cavity is evaluated by using a monopole probe and a transmission line.

A. Evaluation Using a Monopole Probe

The monopole probe is set in the position of the center of the cavity wall as shown in Fig. 1(b). At this location, the x-component of the electric field E_x and the output of the probe is a maximum when the dominant TE_{011} mode is generated in the cavity. The cavity resonates at 492 MHz for the dominant TE_{011} mode, where the susceptibility becomes higher. Therefore, the susceptibility evaluation of the cavity is conducted at this frequency.
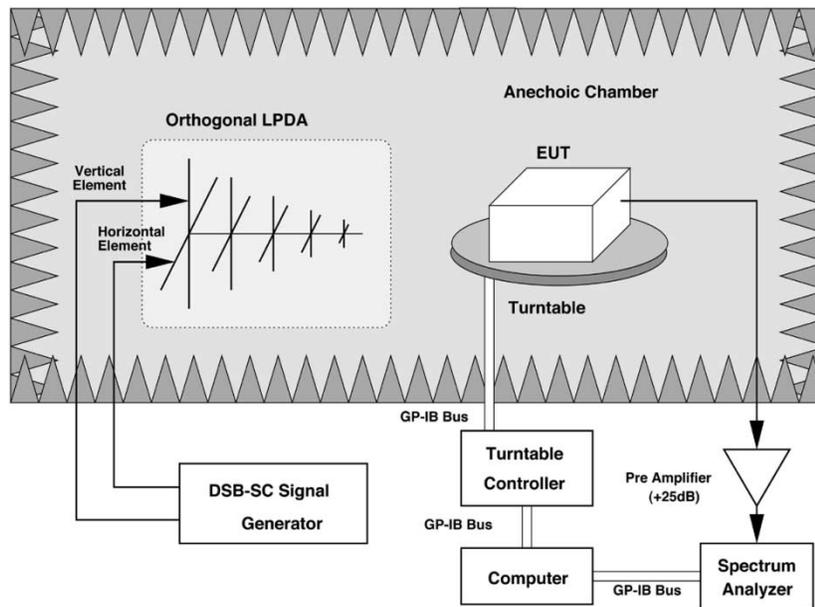
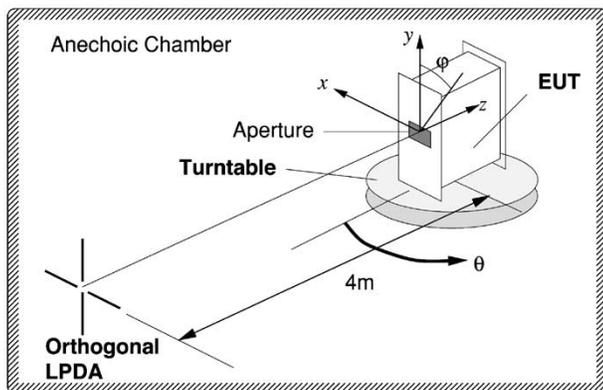Fig. 3.   Schematic representation of the test setup.

Fig. 4.   Overview of the test site coordinates and EUT rotation.

The 3-D susceptibility maps of Cavity #1 shown in Fig. 5(a), are shown in Fig. 6 for the computed and measured results. Fig. 6(a) shows the susceptibility of the cavity calculated by the FDTD method using the reciprocity theorem. The numerical calculations are performed to 65 000 time steps. Approximately 35 h in total on a single PC (Pentium4: 2 GHz, 1-GB memory) were required. A comparison of the measured and modeled results for a specific cut of the 3-D susceptibility map at $\varphi = 90°$ is shown in Fig. 7. The distinguishing characteristics such as the series of gently sloping, broad peaks are obtained in both results. The difference of the experimental and numerical results is less than 2.5 dB. It is thought that this is due to the horizontal position of the LPDA and EUT being slightly out of alignment. One surprising feature is that excitation from the direction opposite the aperture, $\theta = 180°$, results in a field level that is only approximately 7 dB less than with the field incident from the side with the aperture, $\theta = 0°$. From reciprocity, the radiation to the rear of the cavity is also at a relatively high level.

Fig. 8 shows the susceptibility map for Cavity #2 in Fig. 5(b), which has an aperture at a right angle relative to the aperture direction of Cavity #1. The susceptibility map is similar to that for Cavity #1, and the highest susceptibility results when $\varphi = 90°$ and $270°$, similar to that for Cavity #1. This fact suggests that the susceptibility would be greatest when the exciting direction is coincident with the direction of the dominant electric field interior to the cavity, regardless of the aperture direction, and similarly, for radiation, the level would become high in such directions as well. Of course, this statement is for the dominant mode of the model configuration, but some comments may be added for a general resonant mode, for example, the electric field may not be excited at all if the aperture is located in the null direction of some resonant mode. Fig. 9 shows a comparison of the susceptibility characteristics of Cavity #1 and #2 for $\theta = 0°$. Although, high susceptibility appears in the same exciting direction, the susceptibility levels differ. These levels depend on the exciting efficiency of the cavity mode through the aperture. Therefore, the direction of an aperture affects the exciting efficiency of the cavity mode.

The above results show the susceptibility can be effectively estimated by using FDTD calculation which considered reciprocity. Theoretically, both experimental and numerical evaluations of the susceptibility can be carried out over a wide frequency range. However, pre- and power amplifiers that can be used over a wide band are required. The experiment is not conducted over a wide band due to the circumstances of the measuring instruments.

B. Evaluation Using a Transmission Line

Next, a model for a transmission line in the cavity is considered. In practical applications of shielded cavities for electric or electronic equipment, there exist various transmission-line-like structures such as interconnecting wires, traces on printed
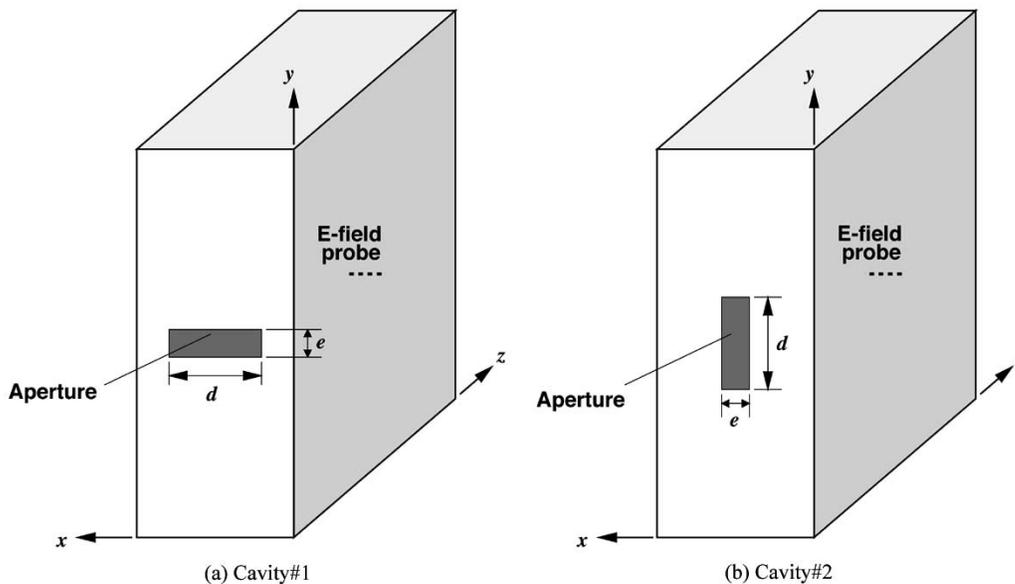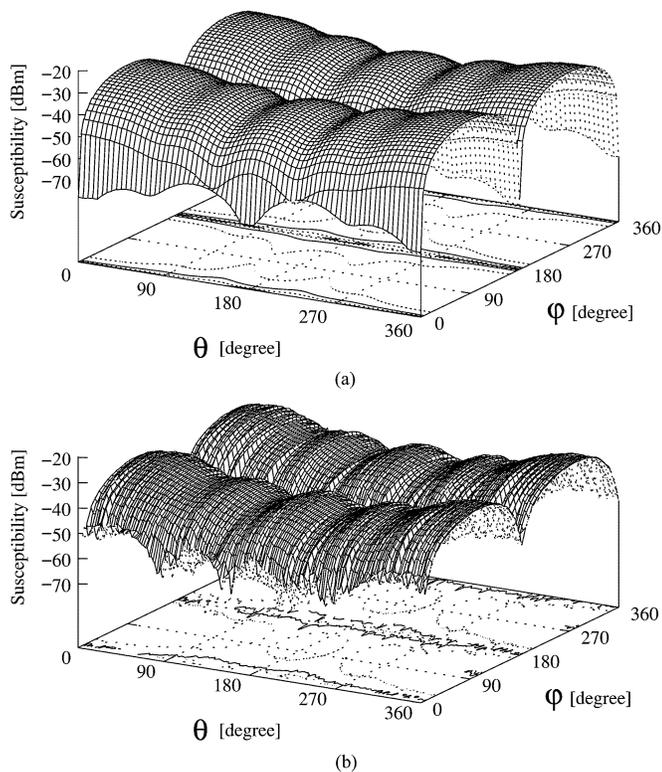
Fig. 5.   Form and position of an aperture.

Fig. 6.   3-D susceptibility map of Cavity #1. (a) Calculated results. (b) Measured results.

Fig. 7.   Comparison between numerical and measured 2-D susceptibility characteristics of Cavity #1 for $\varphi = 90°$. The solid line is for measured results and the dotted line for numerical results.

circuit boards, and so on. When the radiation and susceptibility models for the cavity containing electric circuits and various interconnecting wires in it are considered, such electrically long lines are among the elements to be considered first because of their antenna-like behaviors. The transmission line may play a role of an exciter for radiation and of a mediator for susceptibility.
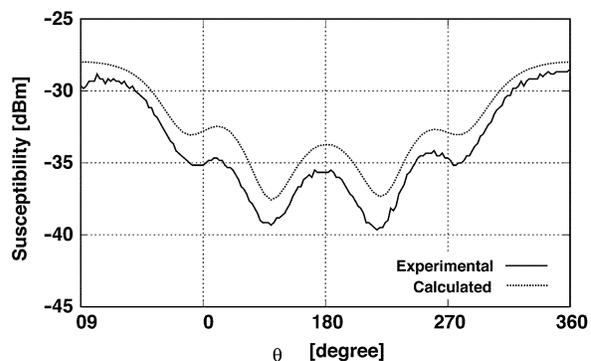
First, a simple model of a wire line is considered, with length $\ell = 90$ mm installed at a height $h = 15$ mm above one cavity wall in the y-z plane, as shown in Fig. 10. The structure at the load terminal is shown in Fig. 11. The diameter of the line is $d = 1$ mm.

For the susceptibility model, the transmission line is terminated in a 50-Ω load, and the other end is terminated in a 50-Ω load or open-circuited. The characteristic impedance of the transmission line is approximately 215 Ω, so that the line system is always unmatched. For the radiation case, the transmission line is fed with a voltage source with an internal resistance of 50 Ω at the same terminal as the one terminated by the 50-Ω load for the susceptibility case.

Fig. 12 shows the 3-D characteristics when the line terminals are located at (0, 165, and 220 mm) and (0, 255 and 220 mm), and terminated by 50-Ω loads. The measurement system is similar to that discussed in Section II-C. The experimental and the computational results are in a good agreement. For other ter-
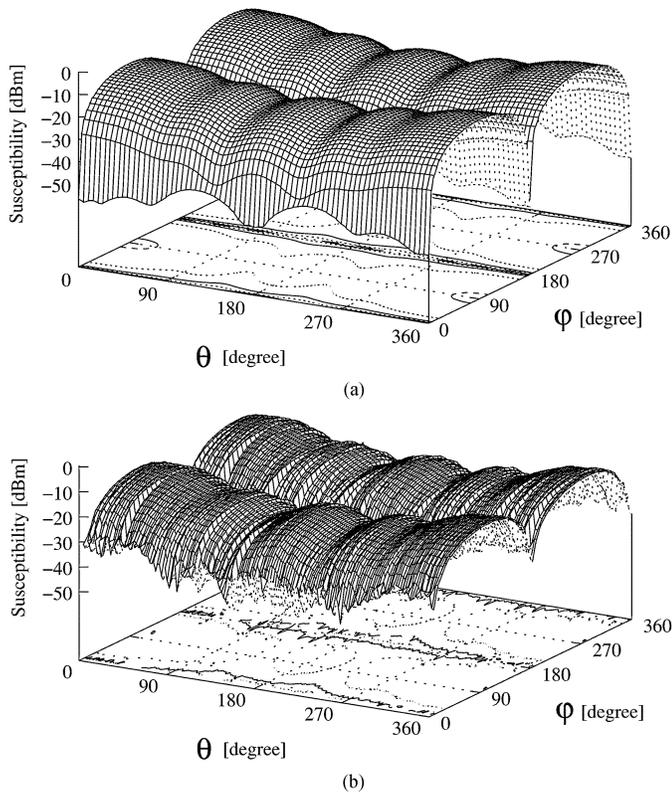
Fig. 8.   3-D susceptibility map of Cavity #2. (a) Calculated results. (b) Measured results.
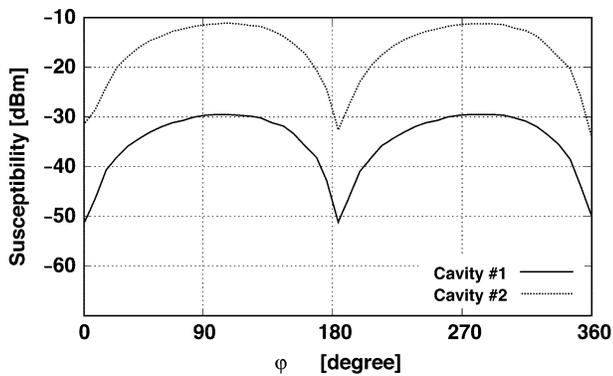

Fig. 10.   Transmission-line signal conductor located above the enclosure wall.
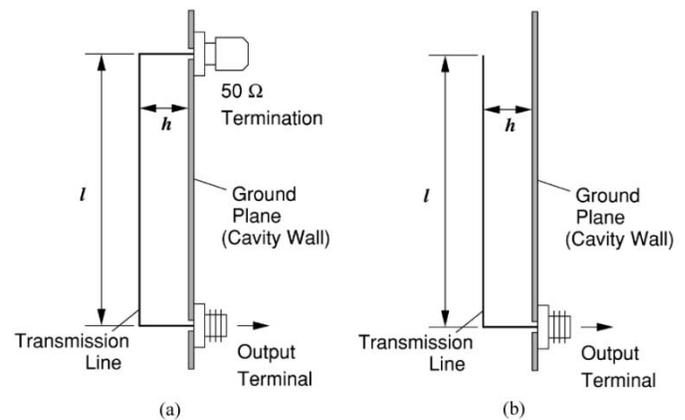
Fig. 11.   Terminal structure of transmission line. (a) 50-Ω load. (b) Open circuit.

Fig. 9.   Comparison between measured 2-D susceptibility characteristics of Cavity #1 and #2 for $\theta = 0°$. The solid line is for Cavity #1 and the dotted line for Cavity #2.

minal conditions mentioned above, the characteristics are similar in pattern, but different in magnitude.

To discuss the differences between the different loading characteristics, the 2-D data for $\theta = 0°$ are shown in Fig. 13, where the horizontal axis denotes the rotating angle of the electric-field direction, φ, and the vertical axis the magnitude. The results for the different loading conditions are similar in pattern but different in magnitude. The difference of levels at $\varphi = 90°$ is discussed here specifically to check the susceptibility mechanism.

To consider the results for differing loading conditions, the characteristics of the transmission line itself are detailed. The susceptibility of a nonmatched transmission line in the cavity would depend on whether the line is at a frequency when the line length corresponds to an integer-multiple of one
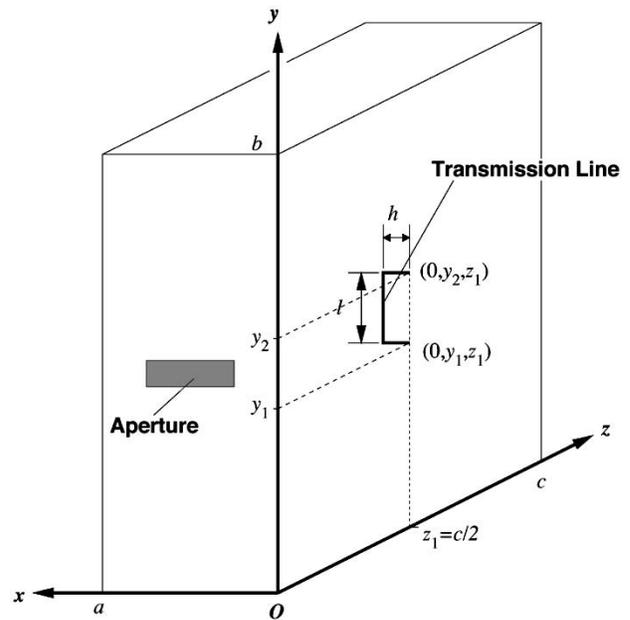
half wavelength. The reflection coefficient characteristics, in terms of S_{11}, of the transmission line in the cavity are shown in Fig. 14. From these results, the minimum level appears at 492 MHz, which corresponds to the dominant mode frequency of the cavity. These results indicate that the highest radiation level would occur at the resonant frequency of the cavity. For the dominant TE_{011} mode, the electric field perpendicular to the y–z plane is a maximum at the center, and decreases gradually with a sinusoidal variation as the observation point moves closer to the conducting side walls of the enclosure. Taking into account this field pattern, the coupling of the fields to the transmission line for the susceptibility case is considered.

The transmission lines modeled here are excited by the electric field normal to the y–z plane and the magnetic field parallel to this plane, which are the components of the TE_{011} mode. Therefore, generally speaking, the coupling is caused by both fields, i.e., electric- and magnetic-field coupling. For the transmission line excited by external fields, the modified telegrapher's equations hold approximately under the condition that
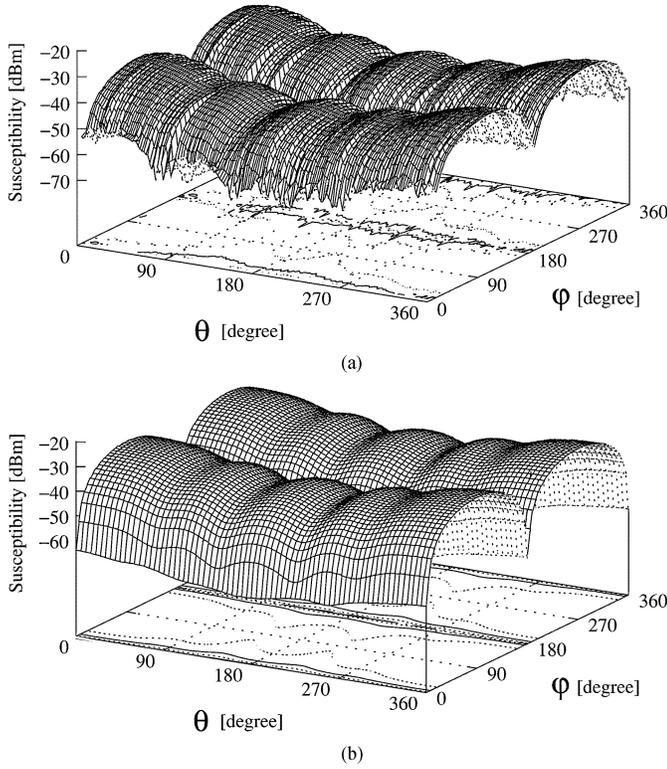
(a)

(b)

Fig. 12. 3-D susceptibility map for the transmission line located on the enclosure wall: $R_0 = R_\ell = 50 \ \Omega$. (a) Experimental results. (b) Numerical results. The line terminals are at $y_1 = 165$ mm, $y_2 = 255$ mm, and $z_1 = 220$ mm.

the cross-sectional dimensions of the transmission line are much smaller than the wavelength involved [12]–[15]. The case here satisfies this condition. From a solution to the modified telegrapher's equations, the induced current at the load can be determined by applying terminal conditions [16], [17]. Letting the current at $y = y_1$ be I_0, then the induced current is

$$I_0 = \frac{h}{\Delta} \left\{ \left(\cos \beta \ell + j \frac{R_\ell}{Z_0 \sin \beta \ell} \right) E_x^e(0, y_1, z_1) \right.$$
$$\left. - E_x^e(0, y_2, z_1) \right\} \quad (2)$$

with

$$\Delta = (R_0 + R_\ell) \cos \beta \ell + j \left(Z_0 + \frac{R_0 R_\ell}{Z_0} \right) \sin \beta \ell \quad (3)$$

where the line height h is assumed as very small compared with the wavelength involved, and Z_0 and β are, respectively, the characteristic impedance and the phase constant of the line. The term $E_x^e(x, y, z)$ denotes the x component of the exciting electric field at point (x, y, z). The induced current I_ℓ at $y = y_2$ can be obtained by changing y_1 to y_2 and *vice versa* on the right-hand side of (2).

From (2), it is seen that I_0 and I_ℓ are of the same level when the center of the transmission line installed along the y direction corresponds to the center of the cavity, because the electric fields at both line terminals are the same in the cavity. Moreover,
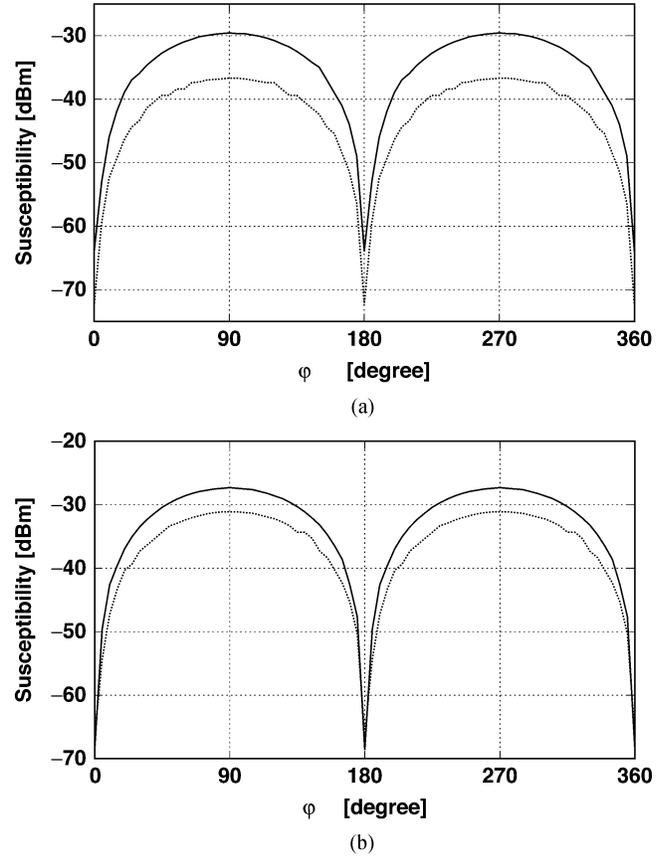

(a)

(b)

Fig. 13. 2-D susceptibility characteristics for $\theta = 0$. (a) Comparison between those due to different line positions for $R_0 = R_\ell = 50 \ \Omega$. The solid line is for $y_1 = 175$ mm and $y_2 = 265$ mm, and the dotted line for $y_1 = 325$ mm and $y_2 = 415$ mm. (b) Comparison between those due to terminals when the line is open-circuited. The line terminals are at $y_1 = 325$ mm and $y_2 = 415$ mm; the solid line is for an open circuit at y_2, and the dotted line at y_1.
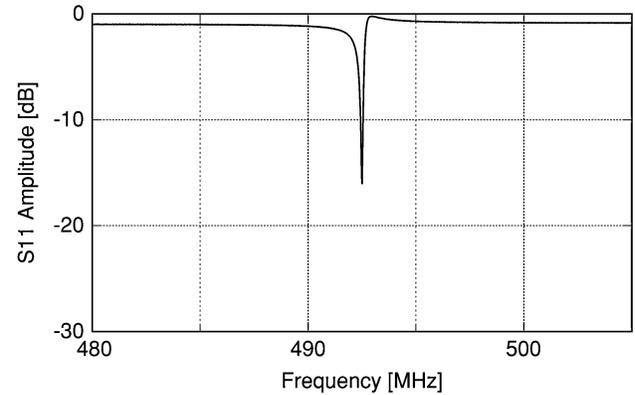
Fig. 14. Measured $|S_{11}|$ characteristics of the 50-Ω terminated transmission line in the cavity.

if the electric fields at both line terminals are different, the induced currents are different. These facts can be confirmed from Fig. 13, and are further examined for the open-circuit case.

For the open-circuit termination, that is, R_ℓ goes to infinity for example, I_0 is

$$I_0(R_\ell = \infty) = \frac{jh E_x^e(0, y_1, z_1) \sin \beta \ell}{Z_0 \cos \beta \ell + j R_0 \sin \beta \ell}. \quad (4)$$

This signifies that the induced current depends on the exciting electric field at the opposite line terminal or the open terminal. Comparing I_0 and I_ℓ for the open-circuit termination

$$\frac{I_\ell(R_0 = \infty)}{I_0(R_\ell = \infty)} = \frac{E_x^e(0, y_2, z_1)}{E_x^e(0, y_1, z_1)}. \tag{5}$$

Therefore, if $E_x^e(0, y_1, z_1)$ is greater than $E_x^e(0, y_2, z_1)$, I_0 is greater than I_ℓ. In our model, by supposing the exciting field sinusoidally distributed over the length of the line, the level differences are reasonable as shown in Fig. 13(b). From these considerations, it can be concluded that the transmission line plays a significant role, which depends strongly on the locations of the terminals. The greater that the field at the terminal position is, the higher the radiation/susceptibility occurs.

IV. CONCLUSION

The susceptibility characteristics of a cavity with apertures using slowly rotating EM fields has been investigated. The FDTD method for the numerical analysis of the susceptibility, where the reciprocity theorem was applied, has been used. Since the 3-D susceptibility characteristics are obtained in only one FDTD run, the computation time is greatly minimized. The experiments were conducted using a developed susceptibility test method with rotating EM fields. The results of the FDTD analysis agree well with the results of the measurements. For a cavity loaded with a transmission line, the susceptibility of the transmission line depends greatly on the terminal conditions of the transmission line and its position as well. Thus for a given enclosure, the susceptibility of a victim circuit inside it can be reduced by adjusting the position of the circuit. Based on the 3-D susceptibility map of the loaded enclosure, obtained either experimentally or numerically, an enclosure with high shielding capability can be designed.

REFERENCES

[1] H. A. Méndez, "Shielding theory of enclosures with apertures," *IEEE Trans. Electromagn. Compat.*, vol. EMC-20, pp. 296–305, May 1978.

[2] M. P. Robinson, T. M. Benson, C. Christopoulos, J. F. Dawson, M. D. Ganley, A. C. Marvin, S. J. Porter, and D. W. P. Thomas, "Analytical formulation for the shielding effectiveness of enclosures with apertures," *IEEE Trans. Electromagn. Compat.*, vol. 40, pp. 240–248, Aug. 1998.

[3] W. Wallyn, F. Olyslager, E. Laermans, D. De Zutter, R. De Smedt, and N. Lietaert, "Fast evaluation of the shielding efficiency of rectangular shielding enclosures," in *Proc. IEEE Int. Symp. Electromagnetic Compatibility*, Seattle, WA, Aug. 1999, pp. 311–316.

[4] M. Li, J. Nuebel, J. L. Drewniak, T. H. Hubing, R. E. DuBroff, and T. P. Van Doren, "EMI from cavity modes of shielding enclosures—FDTD modeling and measurements," *IEEE Trans. Electromagn. Compat.*, vol. 42, pp. 29–38, Feb. 2000.

[5] M. D'Amore and M. S. Sarto, "Theoretical and experimental characterization of the EMP interaction with composite metallic enclosures," *IEEE Trans. Electromagn. Compat.*, vol. 42, pp. 152–163, Feb. 2000.

[6] G. Cerri, R. De Leo, and V. M. Primiani, "Theoretical and experimental evaluation of the electromagnetic radiation from apertures in shielded enclosures," *IEEE Trans. Electromagn. Compat.*, vol. 34, pp. 423–432, Nov. 1992.

[7] G. Caccavo, G. Cerri, V. M. Primiani, and P. Russo, "ESD field penetration into a populated metallic enclosure: A hybrid time-domain approach," *IEEE Trans. Electromagn. Compat.*, vol. 44, pp. 243–249, Feb. 2001.

[8] M. Li, "Modeling and design of shielding enclosures for EMI mitigation—experiments, and finite-difference time-domain and method of moments modeling," Ph.D. dissertation, Univ. Missouri, Rolla, MO, 1999.

[9] L. T. Gnecco, *The Design of Shielded Enclosures: Cost-Effective Methods to Prevent EMI*. Woburn, MA: Butterworth–Heniemann, 2000.

[10] K. Murano and Y. Kami, "A new immunity test method," *IEEE Trans. Electromagn. Compat.*, vol. 44, pp. 119–124, Feb. 2002.

[11] A. Taflove and S. Hagness, *Computational Electrodynamics: The Finite-Difference Time-Domain Method*, 2nd ed. Norwood, MA: Artech House, 2000.

[12] C. D. Taylor, R. S. Satterwite, and C. W. Harrison, "The response of a terminated two-wire transmission line excited by a nonuniform electromagnetic field," *IEEE Trans. Antennas Propagat.*, vol. AP-13, pp. 987–989, June 1965.

[13] C. R. Paul, "Frequency responses of multiconductor transmission lines illuminated by an incident electromagnetic field," *IEEE Trans. Electromagn. Compat.*, vol. EMC-18, pp. 183–190, Nov. 1976.

[14] K. S. H. Lee, "Two parallel terminated conductors in external fields," *IEEE Trans. Electromagn. Compat.*, vol. EMC-20, pp. 288–296, May 1978.

[15] A. K. Agrawal, H. J. Price, and S. H. Gurbaxami, "Transient response of multiconductor transmission lines excited by a nonuniform electromagnetic field," *IEEE Trans. Electromagn. Compat.*, vol. EMC-22, pp. 119–129, May 1980.

[16] Y. Kami and R. Sato, "Circuit-concept approach to externally excited transmission lines," *IEEE Trans. Electromagn. Compat.*, vol. EMC-27, pp. 177–183, Nov. 1985.

[17] Y. Kami, "Mechanism of electromagnetic radiation from a transmission line," *IEICE Trans. Commun.*, vol. E57-B, no. 3, pp. 115–123, Mar. 1992.

Kimitoshi Murano (S'98–M'01) was born in Osaka, Japan, in 1972. He received the B.E., M.E., and D.E. degrees from the University of Electro-Communications, Chofu, Tokyo, Japan, in 1995, 1997, and 2000, respectively.

From 2000 to 2003, he was a Research Associate with the University of Electro-Communications. Since 2003, he has been with the Department of Communications Engineering, Tokai University, Hiratsuka, Japan, where he is currently an Assistant Professor. His research interests include EMC/EMI and maritime radio communications.

Dr. Murano is a Member of the IEICE of Japan.

Takeshi Sanpei was born in Ibaraki, Japan, in 1978. He received the B.E. degree from the University of Electro-Communications, Chofu, Tokyo, Japan in 2000, and is currently working toward the M.E. degree at the same university.

His research interests include EMC/EMI.

Mr. Sanpei is a Member of the IEICE of Japan.

Fengchao Xiao (M'01) was born in Hebei, China, in November 1965. He received the B.E. and M.E. degrees, both in electrical engineering, from Tsinghua University, Beijing, China, in 1987 and 1989, respectively, and the Ph.D. degree from the University of Electro-Communications, Tokyo, Japan, in 1999.

He joined the University of Electro-Communications in April 1999, and is currently working as a Research Associate in the Department of Information and Communication Engineering. His research interests include EMC, numerical methods for solving electromagnetic problems, antenna and microwave circuit analysis and design.

Dr. Xiao is a Member of the IEICE of Japan.

Chen Wang (S'00) received the B.S. and M.S. degrees in electrical engineering, both with honors, from Huazhong University of Science and Technology, Wuhan, China, in 1992 and 1995, respectively, and the Ph.D. degree from the University of Missouri-Rolla in 2004.

From 1995 to 1998, she worked as a Circuit Design Engineer with the Chinese Academy of Sciences, Shanghai Institute of Technical Physics, Shanghai, China. She is currently an SI and EMC Engineer with Nvidia Corporation, Santa Clara, CA. Her current research interests include signal integrity, power integrity, and EMI designs in high-speed digital systems.

Yoshio Kami (M'74) was born in Kagoshima, Japan, in 1943. He received the B.E. degree from the University of Electro-Communications, Chofu, Tokyo, Japan, in 1966, the M.E. degree from Tokyo Metropolitan University, Tokyo, Japan, in 1970, and the D.E. degree from Tohoku University, Sendai, Japan, in 1987.

From 1966 to 1987, he was with the Junior College of Electro-Communications, Chofu, and since 1987, he has been with the University of Electro-Communications where he is currently a Professor.

From May 1999 to May 2001, he was a Chair of the Electromagnetic Compatibility Technical Group of IEICE, and is now serving as an Associate Editor of the IEEE Transaction on Electromagnetic Compatibility and a Chair of the IEEE EMC Society Japan Chapter. His current research interests include EMC/EMI, microwave transmission circuits, and numerical analysis.

James L. Drewniak (S'85–M'90–SM'01) received the B.S., M.S., and Ph.D. degrees in electrical engineering from the University of Illinois at Urbana-Champaign, Urbana, in 1985, 1987, and 1991, respectively.

He joined the Electrical Engineering Department at the University of Missouri-Rolla in 1991, where he is one of the principal faculty members in the Electromagnetic Compatibility Laboratory. His research and teaching interests include electromagnetic compatibility in high-speed digital and mixed signal designs, electronic packaging, and electromagnetic compatibility in power electronic based systems.

Dr. Drewniak is the Chair of the EMC Society Technical Committee TC-10 Signal Integrity.